Preparation and Characterization of Nanostructured *Lillianite* Thin Films

Omar H. Abd-Elkader [1, 2*], S. Mahmoud [2] and N. M. Deraz [3]

[1] Zoology Department, College of Science, King Saud University, Riyadh11451, Kingdom of Saudi Arabia.
[2] Electron Microscope and Thin Films Department, Physics Division, National Research Center, Dokki 12622, Cairo, Egypt.
[3] Physical Chemistry Department, Laboratory of Surface Chemistry and Catalysis, National Research Center, Dokki 12622, Cairo, Egypt.
* Corresponding author email: omabdelkader7@ksu.edu.sa

Abstract: *Lillianite* (Bi_2S_3) $(PbS)_3$ thin films were prepared by thermal evaporation technique. Thin films of *Lillianite* were thermally deposited on to a glass substrate by evaporating *Lillianite* powders that were prepared by ingot method, which most common technique used for growing compounds for the development of thin films. The films are polycrystalline and average crystallite sizes are 20 nm. *Lillianite* thin films have been characterized by X-ray Diffraction (XRD) technique. Surface morphology of the films was studied with a (SEM) and (TEM). The direct transmission spectrum has been measured over range from 300- 2500 nm. The absorption coefficient, extinction coefficient, and optical band gap are calculated.
[Omar H. Abd-Elkader and N. M. Deraz. **Preparation and Characterization of Nanostructured *Lillianite* Thin Films.** *Life Sci J* 2013;10(4):1570-1574]. (ISSN:1097-8135). http://www.lifesciencesite.com. 207

Keywords: *Lillianite* (Bi_2S_3) $(PbS)_3$ Thin Film; Thermal evaporation; Nanostructured; XRD; Optical constant; and optical band gap.

Introduction

In recent years, semiconductive chalcogenides films of different metals have found worldwide application in various fields of science and technology[1]. The utilization of these promising films needs low coast production and pollution-free techniques. Most of these films are important materials for application in various photoelectric and other kinds of devices[2]. Thin films of metal chalcogenides can be deposited on glass, metal, plastics and other substrates by a variety of techniques, such as pyrolysis, sputtering, evaporation and chemical deposition[1, 2]. The system Pb-Bi-S contains several stoichiometric compounds that are stable phases in wide temperature ranges. This system has been investigated using synthetic methods, as well as that many mineral species have been found [3].In the present work, the most favorable results are obtained from a systematic study of the preparation and characterization of thermal evaporated nanostructured *Lillianite* (Bi_2S_3) $(PbS)_3$ thin films on glass substrate. The films obtained were characterized by XRD, SEM, TEM and optical measurements.

2. Materials and Methods

Pure elements Lead (Pb), Bismuth (Bi), and Sulfur (S) of 99.999 % purity were used in the preparation of ingot samples which used in preparation of *Lillianite* (Bi_2S_3) $(PbS)_3$ thermal evaporation thin films. *Lillianite* powder samples were prepared by direct fusion of 5 g quantities of the Pure Pb, Bi, and S elements, it was reacted in sealed, evacuated, silica ampules, and it was sintered for 5 hours at 1123 K. For the sintered samples it was important to maintain a carful control of temperature to prevent partial melting of the materials, these are melted at this temperature inside the impulse, and the ingot is pulled up. The films were deposited on the substrate maintained at room temperature by thermal evaporation method. The vacuum evaporation unit employed in this work was manufactured by Veb Carl Zeiss Jena; model HBA 120/2 Germany. The deposition chamber was evacuated to a residual air pressure of 10^{-9} Torr prior to all deposition experiments. Glass slides cleaned with degreased trichloroethylene, acetone, and ethanol and rinsed with deionized water in an ultrasonic cleaner and finally etched in a 10 % HF solution just before use for the depositions [4], were used as substrate. Tungsten boats were used as vapor source and were aligned to provide a near-normal deposition onto substrates placed at a distance of 8 cm. The thickness of the film was measured using multiple-beam interferometer. All the prepared films were examined by (XRD) measurements using Cu Kα radiation of X-ray diffraction wavelength λ = 0.15406 nm in the scan range 2θ = 4-80°. The formation of nanoparticle was confirmed using transmission electron microscope (TEM, JEOL 1010). Surface morphology was examined by JEOL model JSM – 6380 LA Scanning Electron Microscope (SEM). Optical transmission measurements were performed with UV/VIS Jasco 7800 spectrophotometer.

3. Results and discussion

Conventional thermal evaporation method is being widely used for the growth of binary and ternary compounds because of its simplicity, importance to obtain high quality, pure compound films for most thin film applications. The process of film formation consists of:

1. Transformation of materials into the gaseous state.
2. Transfer of atoms to substrate.
3. Deposition of these particles on the substrate.
4. Rearrangement of their binding on the surface of substrate.

The parameters can control to achieve the objectives set are:

1. The kinetic energy of particles.
2. Rate of the thin film deposition.
3. Sterilized energy applied to the film during growth.
4. Temperature of the Substrates.

Generate thin films have different adhesion, mechanical strength, optical reflectivity, magnetic properties electrical resistivity, and density. The rate of deposition was estimated interferometrically to be approximately 10 nm / sec, for films deposited at room temperature.

1) XRD analysis:

The crystal structures of powder and thin films were studied by X-ray diffraction. Figures (1) and (2) illustrate the X-ray diffraction pattern of *Lillianite* (Bi_2S_3) $(PbS)_3$, powder ingot and thin films on glass substrate maintained at temperature ~ 323 K, the deposited films were heat treated under vacuum at temperature 623 K for 1 hour and 723 K for 4 hours respectively. Single crystals of the high-temperature phases in the (PbS) (Bi_2S_3) system were prepared by chemical transport reactions. The crystal chemistry of these phases has been investigated [5]. Density measurements prove the existence of cation vacancies within the corresponding structures. The structure of the *Lillianite* (Bi_2S_3) $(PbS)_3$ nanoparticle powders and thin films were calculated with the help of Full-prof [6] and Chekcell [7] programs. Crystal structure of *Lillianite* (Bi_2S_3) $(PbS)_3$ were investigated from XRD data by the following steps:

1. Read data Files by Full-prof program.
2. Calculate the diffracted peaks.
3. Calculate the lattice parameters and determine the best space group.
4. Check cells and peaks by checkcell program.

Lillianite (Bi_2S_3) $(PbS)_3$ is formed in the powder and thin films samples as shown as in fig (2), lattice parameters and detailed indexing data are listed in tables (1) and (2).

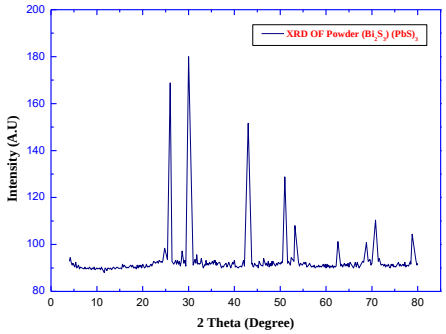

Fig. 1. XRD reflections of powder *Lillianite.*

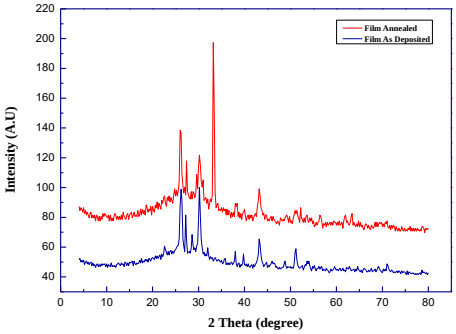

Fig. 2. XRD reflections of *Lillianite*Thin Films.

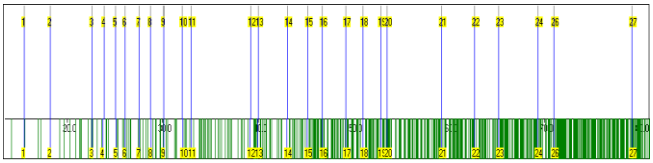

Fig. 3. Measured reflections of (Bi_2S_3) $(PbS)_3$ *Lillianite* with Phase III (Bi_2S_3) $(PbS)_3$.

Table (1) lattice parameters *Lillianite* (Bi_2S_3) $(PbS)_3$ Final values: (standard errors on 2nd line)

a	**13.6708**
standard errors	**0.0010**
b	**31.3183**
standard errors	**0.0024**
c	**4.1350**
standard errors	**0.0003**
α	**90.0000**
standard errors	**0.0000**
β	**90.0000**
standard errors	**0.0000**
γ	**90.0000**
standard errors	**0.0000**
volume	**1770.384**
standard errors	**0.3866**
Space group	**Bbmm**

Table (2) indexing of *Lillianite* (Bi_2S_3) $(PbS)_3$

h	k	l	2θ(Obs)	2θ(Calc)	Diff.
2	3	0	15.490	15.482	0.008
1	6	0	18.191	18.177	0.014
1	1	1	22.626	22.626	0.000
2	7	0	23.876	23.749	0.127
2	0	1	25.046	25.150	-0.104
4	0	0	26.032	26.050	-0.018
0	6	1	27.486	27.496	-0.010
2	9	0	28.710	28.765	-0.055
1	7	1	30.119	30.121	-0.002
1	11	0	32.009	32.085	-0.076
4	7	0	32.937	32.952	-0.015
3	9	1	39.219	39.154	0.065
6	2	0	39.980	39.952	0.028
2	12	1	43.084	43.031	0.053
1	3	2	45.200	45.158	0.042
1	5	2	46.747	46.702	0.045
2	6	2	49.180	49.199	-0.019
7	7	0	50.975	50.980	-0.005
5	14	0	52.820	52.834	-0.014
1	10	2	53.512	53.484	0.028
1	13	2	59.220	59.231	-0.011
3	20	0	62.670	62.683	-0.013
8	12	0	65.185	65.202	-0.017
1	23	0	69.295	69.290	0.005
1	6	3	70.986	71.006	-0.020
1	6	3	70.986	71.006	-0.020
11	6	0	79.159	79.155	0.004

2) The surface morphology studies:

The grains or crystallites are formed by independent nucleation and growth processes randomly oriented and spaced with respect to one another. There is, in general, no epitaxial registration with the substrate lattice other than for nucleation occurring preferentially at defect sites and other surface irregularities. As shown in figure (4) the grain sizes of the films are spherical globules, as interdiffusion takes place, as shown in figure (5) the grains coalesce to give a high lead sulfide concentration, the surface becomes smooth and metallic specks are seen, It was noticed that as the temperature of annealing process increases, the dimensions of the crystallites are not uniform. Figures (4 and 5) show that the small spherical Nano grains of approximately 30-50 nm size were uniformly distributed over the homogeneous background.

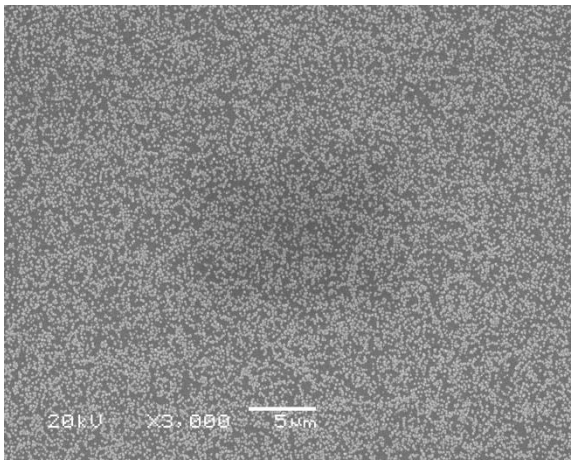

Fig. 4. Surface morphology of *Lillianite* thin films (Bi_2S_3) $(PbS)_3$ a (SEM).

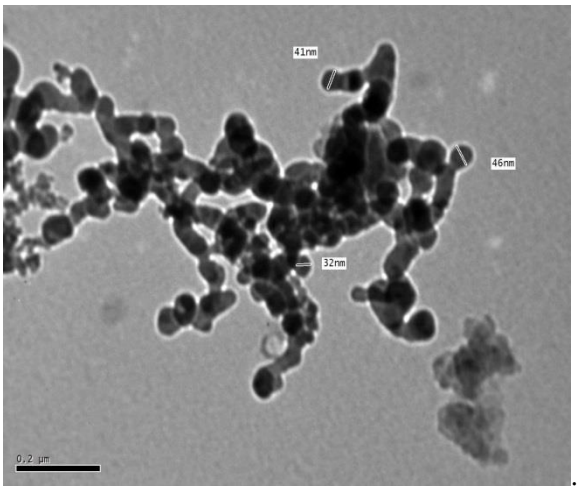

Fig. 5. Surface morphology of *Lillianite* thin films (Bi_2S_3) $(PbS)_3$ a (TEM).

3) The optical properties studies:

The optical constants of a number of semiconductors have been measured over a wide range of wavelengths. Generally in the near or intermediate infra-red, the absorption coefficient drops rapidly and the material becomes fairly transparent at longer wavelengths. This marked drop in absorption is called the fundamental absorption edge. Near the absorption edge, the Coulomb interaction between the free hole and electron must be taken into account, higher energy bands participate in the transition processes, and complicated band structures are reflected in the absorption coefficient [8]. The typical optical transmission (**T**) spectra of *Lillianite* (Bi_2S_3) $(PbS)_3$ thin film were recorded at room temperature in the spectral range (300-2500 nm), which covers the fundamental optical absorption edge and the interband transition region of the semiconductors materials. Figure (6) shows the typical optical transmission

spectrum of as deposited and annealed films, respectively. The transmittance is high in Vis-NIR region and the high transmittance make the film a good material for thermal control window coating for cold climates and anti- reflection coating. The thickness of the films runs from 40 to 140 nm for the films deposited, the results for the roughness of the films surface show low values between 10 and 20 nm.

The effects of annealing in transmission curves can be noteworthy:

- Transmission of the as-deposited samples, showed gradual light absorption in a wide range of optical wavelength (300–500 nm).
- Exponential increase in transmittance with wavelength is observed, which is characteristic of distorted semiconductor.
- The optical absorption edge of the of *Lillianite* (Bi_2S_3) $(PbS)_3$ films was shifted toward a longer wavelength side with increase of PbS content.
- This indicates that the optical bandgap of these semiconductors linearly decreases from 1.92 eV (Bi_2S_3) to 0.4 eV (PbS) [9].

Figure (7) shows the absorption coefficient (**α**) and Figure (8) shows the extinction coefficient (**k**) calculated from Equations. (1), and (2) for the *Lillianite* (Bi_2S_3) $(PbS)_3$. The extinction coefficient (k) increases gradually with photon energy.

$$\alpha\ (h\ \nu) = 1/d\ \ln\ 1/T \qquad (1)$$

Where **d** is the thickness of the films, and **T** is the transmission. The absorption coefficient **α** is related to the extinction coefficient **k** by[10]:

$$k = \alpha\lambda/4\pi I \qquad (2)$$

Figure (9) shows the optical band gap calculated from the measured Transmission using the following relation [11, 12]. Equation (3).

$$\alpha = A\ (h\upsilon - E_g)^{m} \qquad (3)$$

Where A is constant and m = 1/2 or 2 for an allowed direct or indirect transition energy gap. The direct E_g were obtained from linear portion of (α^2) vs. (**h ν**) plot, through the intersection of the straight line with the axis of the photon energy and it is found in range 1.27 eV. It is clearly seen from the optical spectrum an absorption edge shift toward a lower wavelength in the films. This property makes it an excellent candidate for opto-electronic applications in many fields such as photography, IR detectors, solar absorbers, light emitting devices and solar cells.

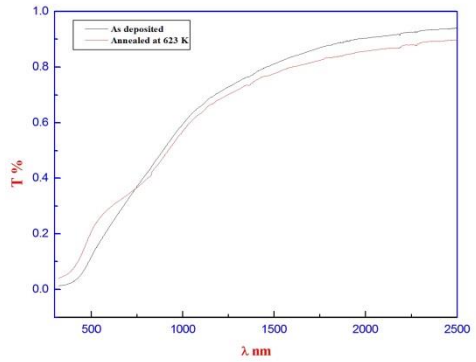

Fig. 6. Optical transmission of *Lillianite* thin films (Bi_2S_3) $(PbS)_3$.

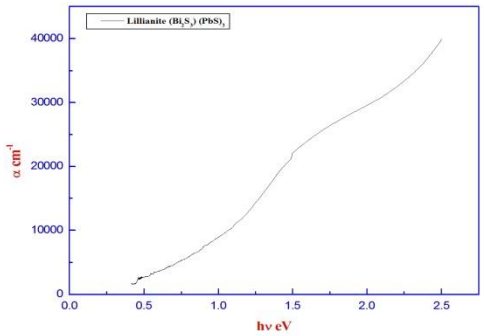

Fig. 7. Absorption coefficient of *Lillianite* thin films (Bi_2S_3) $(PbS)_3$.

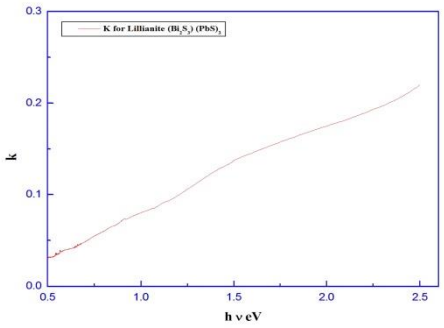

Fig. 8. Extinction coefficient of *Lillianite* thin films (Bi_2S_3) $(PbS)_3$.

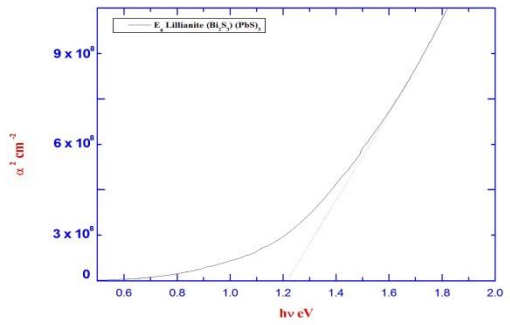

Fig. 9. Calculated optical band of *Lillianite* thin films (Bi_2S_3) $(PbS)_3$.

Acknowledgments

"The authors would like to extend their sincere appreciation to the Deanship of Scientific Research at King Saud University for its funding of this research through the research Group projects no RGP-VPP-306 ".

Conclusions:

In summary, we have prepared (Bi_2S_3) $(PbS)_3$ *Lillianite* thin films by thermal evaporation technique. The grain size lies in the interval of 20-50 nm. We calculate the lattice parameters, space group and crystal structure. Surface Morphology shows that the small spherical nanograins were uniformly distributed over the smooth homogeneous background of crystalline phase. The high transmittance makes a film a good material for thermal control window coating for cold climates and anti- reflection coating. Optical absorption spectra are quantified for the *Lillianite* in which the redshift of E_g is associated with the decrease of the average grain size. Direct band gap energy (E_g) in the range of 1.27 eV.

Corresponding Author:
Dr. Omar Hamed Abd Elkader
Associated Prof. Electron Microscopy**.**
Electron Microscope Unit, Zoology Department, College of Science, King Saud University**.**

E-mail: omabdelkader7@ksu.edu.sa

References:

1. S. Mahmoud, and H. Omar, FIZIKA A 10 1, 21-30 (2001).
2. S. Mahmoud, A. H. Eid, and H. Omar, FIZIKA A 6 3, 111–120(1997).
3. K.M. Gadaves, S.A.Jodgudri and C.D.Lokhande, Thin Solid Films, 245,7(1994).
4. H. Omar Abd Elkader, International Conference on Fundamental and Applied Sciences (ICFAS 2012) Kuala Lumpur, Malaysia12th to 14th June (2012).
5. H.H Otto and H.Strunz, N.Jb.Miner.Abh.108 (1), 1(1968)'.
6. D.B. Wiles & R.A. Young, J. Applied Cryst. 14, 149 (1981).
7. Altermatt and Brown in Acta Cryst. A34, 125-130 (1987).
8. Y. Wang, A. Suna, W. Mahler, R. Kasowski, J. Chem. Phys. 87 7315(1987).
9. D.K. Schroder, Semiconductor Material and Device Characterization, Wiley, New York, p. 597 (1990).
10. R. E. Denton, R. D. Campbell and S. G. Tomlin, J. Phys. D. Appl. Phys. 5 852 (1972).
11. S. Isomura, S. Shirakata, and T. Abe, Solar Energy Materials Vol. 22 P. 223 (1991).
12. M. Susama, and H.C. Padhi, J. Appl. Phys Vol.75 (9), 4576 – 4580, (1994).

10/22/2013